Tetracaine hydrochloride induces macrophage pyroptosis through caspase-1/11-GSDMD signaling pathways

RAN ZHANG[1,2*], WANRONG GOU[1,2*], PENG YI[1,2], ZHENGSHAN QIN[1,2], DANLI ZHU[1,2], JING JIA[1,2], LI LIU[1,2], XIAN JIANG[1-3] and JIANGUO FENG[1,2]

[1]Department of Anesthesiology, The Affiliated Hospital of Southwest Medical University; [2]Anesthesiology and Critical Care Medicine Key Laboratory of Luzhou, Department of Anesthesiology, Southwest Medical University; [3]Department of Anesthesiology, Luzhou People's Hospital, Luzhou, Sichuan 646000, P.R. China

Received March 29, 2023; Accepted June 29, 2023

DOI: 10.3892/etm.2023.12127

Abstract. Tetracaine hydrochloride (TTC) is a long-lasting local anesthetic commonly used for topical anesthesia. Inappropriate dosage or allergic reactions to TTC can lead to local anesthetic toxicity. TTC exerts cytotoxic effects on certain cell types by inducing apoptosis and necrosis; however, the effects of TTC on macrophages are currently unclear. In the present study, the RAW 264.7 and BV2 cell lines, and murine peritoneal macrophages, were used to evaluate the cytotoxicity of TTC. The present study demonstrated that TTC caused a decrease in cell viability according to a Cell Counting Kit-8 assay, increased lactate dehydrogenase and IL-1β secretion according to ELISA, and induced morphological changes characteristic of pyroptosis according to western blotting. Moreover, TTC-induced macrophage pyroptosis was mediated by gasdermin (GSDM)D, and the cleavage of GSDMD was modulated by both caspase-1 and caspase-11. These results were experimentally validated using caspase-1 and caspase-11 inhibitors. Furthermore, it was observed that TTC and lipopolysaccharide (LPS) exerted similar effects on macrophages. However, the mechanism of induction of pyroptosis by TTC was different from that of LPS. The present study demonstrated that TTC alone could induce macrophage pyroptosis mediated by canonical and non-canonical inflammatory caspases. Therapies targeting pyroptosis may potentially provide a promising future strategy for the prevention and treatment of local anesthetic toxicity induced by TTC.

Correspondence to: Ms. Xian Jiang or Dr Jianguo Feng, Department of Anesthesiology, The Affiliated Hospital of Southwest Medical University, 25 Taiping Street, Luzhou, Sichuan 646000, P.R. China
E-mail: jiangxian@swmu.edu.cn
E-mail: fengjianguo@swmu.edu.cn

*Contributed equally

Abbreviations: Beln, Belnacasan; LDH, lactate dehydrogenase; LPS, lipopolysaccharide; TTC, tetracaine hydrochloride; Wede, Wedelolactone

Key words: caspase-1, caspase-11, gasdermin D, pyroptosis, macrophage, tetracaine hydrochloride

Introduction

Local anesthetics exert their analgesic effect by blocking Na^+ channels, thereby affecting the conduction of nerve impulses. They are widely used in clinics as they are safe, exhibit fewer complications than general anesthetics and have minimal impact on physiological functions. However, side effects of local anesthetics can occur, such as local anesthetic allergy and toxicity, which may impact the cardiovascular and central nervous systems (1). These side effects are a result of a combination of adverse effects on ionotropic and metabotropic cell signaling, as well as energy transduction (2). The neurotoxic effects of local anesthetics may include apoptosis, inhibition of voltage-dependent calcium channels, calcium depletion in the endoplasmic reticulum, mitochondrial dysfunction and DNA damage (3,4). Nevertheless, the mechanism underlying toxicity exerted by local anesthetics requires further study.

Tetracaine hydrochloride (TTC) is a long-lasting local anesthetic commonly used for topical anesthesia, which is water-soluble, has strong penetrability and a good anesthetic effect (5). However, TTC has a higher cytotoxicity compared with other local anesthetics due to its high permeability (6). Previous studies have reported that TTC exerts a cytotoxic effect on certain cell types, such as human corneal stromal cells and human corneal epithelial cells, inducing apoptosis and necrosis (7,8). Koizumi *et al* (9) reported that large doses of intrathecal TTC increase the concentration of glutamate in cerebrospinal fluid, thereby causing neuronal injury in rabbits. In addition, AMPA receptor activation was revealed to be involved in TTC-induced neurotoxicity in the spinal cord. Song and Fan (7) reported that TTC-induced apoptosis may be triggered through Fas death receptors and mediated by Bcl-2 family proteins, in a mitochondria-dependent pathway. Pang and Fan (8) reported TTC-induced human corneal epithelial (HCEP) cell apoptosis via a death receptor-mediated mitochondrion-dependent pathway. Werdehausen *et al* (6) reported that low concentrations of TTC induced the apoptosis of human T-lymphoma cells, whereas a higher concentration of

TTC induced necrosis. However, the effect of TTC on macrophages has not currently been fully revealed. Furthermore, whether TTC cytotoxicity involves mechanisms such as pyroptosis is also yet to be elucidated.

Macrophages are specialized, long-lived, phagocytic cells of the innate immune system that are widely distributed in certain tissues and organs of the body, such as the lungs, liver and brain. Macrophages have myriad functions, including eliminating pathogens, promoting tissue development and wound repair, and regulating immunity, metabolism and apoptosis. Additionally, they serve a crucial role in environmental homeostasis and the inflammatory microenvironment (10). A number of previous studies on the central nervous system toxicity of local anesthetics focused on neurons, rather than the immune system (11,12). The present study used a central nervous system immune cell line, the murine microglial cell line BV2, which has a dual effect on neurons. First, they can protect neurons by phagocytosing pathogens and other harmful agents present in the brain tissue. Secondly, under the stimulation of inflammatory factors, they can be activated and secrete inflammatory cytokines, thereby exerting a toxic effect on neurons (13). In addition, the murine macrophage cell line RAW 264.7 and mouse peritoneal macrophages (PMs) were used in the present study to investigate the relationship between TTC and macrophages.

Pyroptosis, also known as gasdermin (GSDM)-mediated programmed necrosis, is a form of pro-inflammatory programmed cell death (PCD) triggered by perturbations of extracellular or intracellular homeostasis related to innate immunity (14). It is initiated by inflammasome activation, which serves a critical role in the defense of hosts against danger signals (9). Pyroptosis is induced by members of the GSDM superfamily, which consist of GSDMA, B, C, D and E, and DFNB59; however, there is no GSDMB gene encoded in the mouse genome. Except for DFNB59, all of the GSDM protein family members possess an N-terminal pore-forming domain and a C-terminal auto-inhibitory domain (15,16). The GSDM proteins initiate proinflammatory cell death via their pore-forming domain after its cleavage by upstream inflammatory caspases (15,16). GSDMD and GSDME are GSDM family proteins that have been widely studied in the context of pyroptosis (17,18). GSDMD-dependent pyroptosis is regulated through a canonical inflammasome pathway, which is activated by caspase-1. Similarly, activation of murine caspase-11 and human caspase-4/-5 is involved in the noncanonical inflammasome pathway (18). GSDME-dependent pyroptosis is activated by apoptotic caspase-3 (17). Through the release of IL-1β and IL-18, pyroptotic cells recruit additional inflammatory cells and induce a cascade of inflammatory responses (19). Pyroptosis is characterized by the formation of a plasma membrane pore, swelling of the cell, rupture of the plasma membrane and the subsequent release of intracellular contents (15). This form of cell death is mainly observed in professional phagocytes, such as macrophages, monocytes and dendritic cells, but emerging evidence suggests that pyroptosis can also be induced in cancer cells (20). Previous studies have reported that pyroptosis serves a significant role in macrophage-induced inflammation (21,22). Inflammatory responses are beneficial to humans as they help remove pathogenic microorganisms and antagonize infection, and the release of cytokines may contribute to tissue angiogenesis (23). However, hyperactivated pyroptosis can result in the induction of a substantial inflammatory cascade leading to tissue and organ damage, thereby causing inflammatory diseases, such as lung inflammatory disease, cardiovascular disease and kidney disease (24).

Previous reports have indicated that TTC can cause allergic reactions and local anesthetics may have antibacterial effects, suggesting a potential effect of TTC on macrophages (25,26). However, the effects of TTC on macrophages and whether pyroptosis is involved in this process have not yet been reported. The present study aimed to find the relationship between TTC and macrophage pyroptosis, and provide a novel mechanism underlying the local anesthetic toxicity of TTC. The findings may point to future novel treatments for local anesthetic toxicity caused by TTC.

Materials and methods

Cell culture. The murine macrophage cell line RAW 264.7 and the murine microglial cell line BV2 were purchased from Procell Life Science & Technology Co., Ltd. (cat. nos. CL-0190 and CL-0493, respectively). RAW 264.7 and BV2 cells were cultured in RAW 264.7-specific medium (cat. no. CM-0190; Procell Life Science & Technology Co., Ltd.). and BV2-specific medium (cat. no. CM-0493; Procell Life Science & Technology Co., Ltd.) with 10% FBS and 1% P/S antibiotics, respectively. Cells were incubated in a humidified incubator at 37˚C with 5% CO_2.

Cells were treated with TTC (H20084308, Chengdu Tiantaishan Pharmaceutical Co. Ltd.) at a range of concentrations from 100 to 400 μM for 24 h at 37˚C, with or without pretreatment with the caspase-1 inhibitor, Belnacasan (Beln) (10 μM; cat. no. HY-13205; MedChemExpress) and/or the caspase-11 inhibitor, Wedelolactone (Wede) (20 μM; cat. no. HY-N0551; MedChemExpress) for 30 min at 37˚C to induce the macrophages, LPS (10 μg/ml; cat. no. L6529; Sigma-Aldrich; Merck KGaA) was added 6 h before TTC treatment.

Light microscopy. RAW 264.7 and BV2 cells were cultured in 100 mm plates (cat. no. 704002; Wuxi NEST Biotechnology Co., Ltd.) in a humidified incubator at 37˚C with 5% CO_2. Once the cells reached the logarithmic growth phase, the medium was replaced with fresh medium containing TTC at concentrations ranging from 100-400 μM for 24 h at 37˚C. The morphology and confluence of the cells were monitored with a light microscope.

Western blotting. The cells were homogenized in RIPA buffer (cat. no. P0013C; Beyotime Institute of Biotechnology), and the protein concentration was determined using a bicinchoninic acid protein assay kit (cat no. PC0020; Beijing Solarbio Science & Technology). Equal quantities of cell lysate (20 μg/lane) were separated by SDS-PAGE on a 10 or 12% gel and then transferred to a 0.45-μm polyvinylidene difluoride membrane. Membranes were blocked with 5% skim milk at room temperature for 1 h, then incubated with primary antibodies against GSDMA (cat no. sc-376318; 1:100; Santa Cruz Biotechnology, Inc.), GSDMC (cat. no. 27630-1-AP; 1:1,000;

Proteintech Group, Inc.), GSDMD (cat. no. ab209845; 1:1,000; Abcam), GSDME (cat. no. ab215191; 1:1,000; Abcam), caspase-1 (cat. no. ab179515; 1:1,000; Abcam), caspase-11 (cat. no. ab180673; 1:1,000; Abcam), caspase-3 (cat. no. 9662; 1:1,000; Cell Signaling Technology, Inc.), and β-actin (cat. no. 66009-1-Ig; 1:10,000; Proteintech Group, Inc.) at 4˚C overnight. Subsequently, the membranes were washed with 1X TBST (0.5% Tween) three times for 10 min and incubated with HRP-conjugated Affinipure goat anti-mouse IgG (H+L) secondary antibodies (cat. no. SA00001-1; 1:10,000; Proteintech Group, Inc.) or HRP-conjugated Affinipure goat anti-rabbit IgG (H+L) secondary antibodies (cat. no. SA00001-2; 1:10,000; Proteintech Group, Inc.) for 1 h at room temperature. After washing with 1X TBST three times for 10 min, the bands were visualized using the ECL FemtoLightChemiluminescence kit (cat. no. PE100; Chengdu Wanda Biotechnology Development Co., Ltd.). To better show the expression levels of the full-length and cleaved forms of the detected proteins, both short and long exposure images are presented in the present study. For relative protein expression quantification, the integrated optical density of the protein bands was assessed using ImageJ software (version 1.31; National Institutes of Health).

Cell Counting Kit-8 (CCK-8) assay. Cell viability was measured using the CCK-8 assay kit (Dojindo Laboratories, Inc.) according to the manufacturer's instructions. RAW 264.7 and BV2 cells were seeded in 96-well plates ($1x10^3$ cells/well) and treated with 100-400 μM TTC, then incubated at 37˚C with 5% CO_2. After 24 h, 10 μl CCK-8 reagent was added to each well, and the cells were further incubated for 1 h at 37˚C. Subsequently, the absorbance of samples was measured at 450 nm using a microplate reader.

ELISA. ELISA was used to measure the levels of IL-1β present in the cell culture medium The cell culture medium was centrifuged at 1,000 x g for 10 min at 4˚C and the levels of IL-1β present were measured using the mouse IL-1β ELISA Kit (cat. no. KE10003; Proteintech Group, Inc.) according to the manufacturer's protocol. A total of 200 μl cell culture medium was loaded into each well of the ELISA plate. The absorbance of each sample was measured at 450 nm using a microplate reader. Standard curves were established using IL-1β standard samples provided in the kit and the concentration of the cytokines in the collected medium was measured.

Lactate dehydrogenase (LDH) release assay. The release of LDH from the cells was measured using the LDH cytotoxicity assay kit (cat. no. C0016; Beyotime Institute of Biotechnology). RAW 264.7 and BV2 cells were seeded in 96-well plates ($1x10^3$ cells/well) and treated with 100-400 μM TTC for 24 h at 37˚C. After treatment, cells were centrifuged at 400 x g for 5 min at 4˚C, then 120 μl supernatant was collected and analyzed using the assay kit according to the manufacturer's instructions. Briefly, 60 μl LDH determination working solution was added to the supernatant and incubated for 30 min at 37˚C. Subsequently, the absorbance of samples was measured at 490 nm using a microplate reader. All experiments were performed in triplicate.

Extraction of murine PMs. The study was approved by the Ethical Approval for Research Involving Animals in Southwest Medical University (Luzhou, China; approval no. SWMU20220028) and all animal experiments were performed according to the Guide for the Care and Use of Laboratory Animals of the National Institutes of Health. A total of 40 male C57BL/6 mice (weight, ~20 g; age, 6-8 weeks) were purchased from Chongqing Tengxin Biotechnology Co., Ltd., and were kept in the Experimental Animal Center of Southwest Medical University. The animals were supplied with food and water *ad libitum* and maintained in a 12/12-h light/dark cycle for 2 weeks (ambient temperature, 22-26˚C; relative humidity, 40-60%). Mice were intraperitoneally injected with TTC (2.5 mg/kg) or an equal volume of physiological saline once a day for 3 consecutive days. Then, PMs were isolated as previously reported (18). First, the mice were euthanized by cervical dislocation and soaked in 70% ethanol for 3 min, then transferred to a clean bench. Subsequently, a small incision was made along the ventral aspect of the mouse abdomen with a sterile scalpel and the abdominal skin was carefully removed to expose the peritoneum. Subsequently, using a 5-ml syringe and a needle, 5 ml RPMI medium 1640 (Gibco; Thermo Fisher Scientific, Inc) supplemented with 1% penicillin/streptavidin was injected into the abdomen. The abdomen was gently massaged and the medium was recovered into a 15-ml tube. Then, the medium was centrifuged for 5 min at 4˚C at 310 x g to pellet the cells. The supernatant was discarded and the cells were resuspended in 1 ml complete RPMI medium. Next, the collected cells were transferred to cell plates and cultivated in complete RPMI medium in a humidified incubator with 5% CO_2 at 37˚C. After being incubated for 1 h, only macrophages adhered to the culture dish. The culture supernatant containing other cells was removed and replaced with fresh culture medium. Then macrophages were then used for the subsequent experiments.

Statistical analysis. Statistical analysis was performed using GraphPad Prism software (version 8.0; Dotmatics). Each experiment was performed in triplicate. Data are presented as the mean ± standard error of the mean. Statistically significant differences were determined by one-way ANOVA followed by Tukey's post hoc test. $P<0.05$ was considered to indicate a statistically significant difference.

Results

TTC induces pyroptosis in macrophages. The cytotoxicity of various concentrations of TTC in RAW 264.7 and BV2 cells was evaluated. Cell viability was measured using a CCK-8 assay and the morphology of cells was observed using a light microscope. The viability of both RAW 264.7 and BV2 cells was significantly decreased by TTC in a dose-dependent manner (Fig. 1A and B). Furthermore, both RAW 264.7 and BV2 cells treated with >200 μM TTC for 24 h underwent morphological alterations. The dying cells showed marked swelling with large bubbles emanating from the plasma membrane (Fig. 1G). These morphological changes were reminiscent of pyroptosis, as reported previously (15). In addition to morphological changes, pyroptosis is characterized by the release of certain inflammatory factors. The levels of secreted LDH and IL-1β

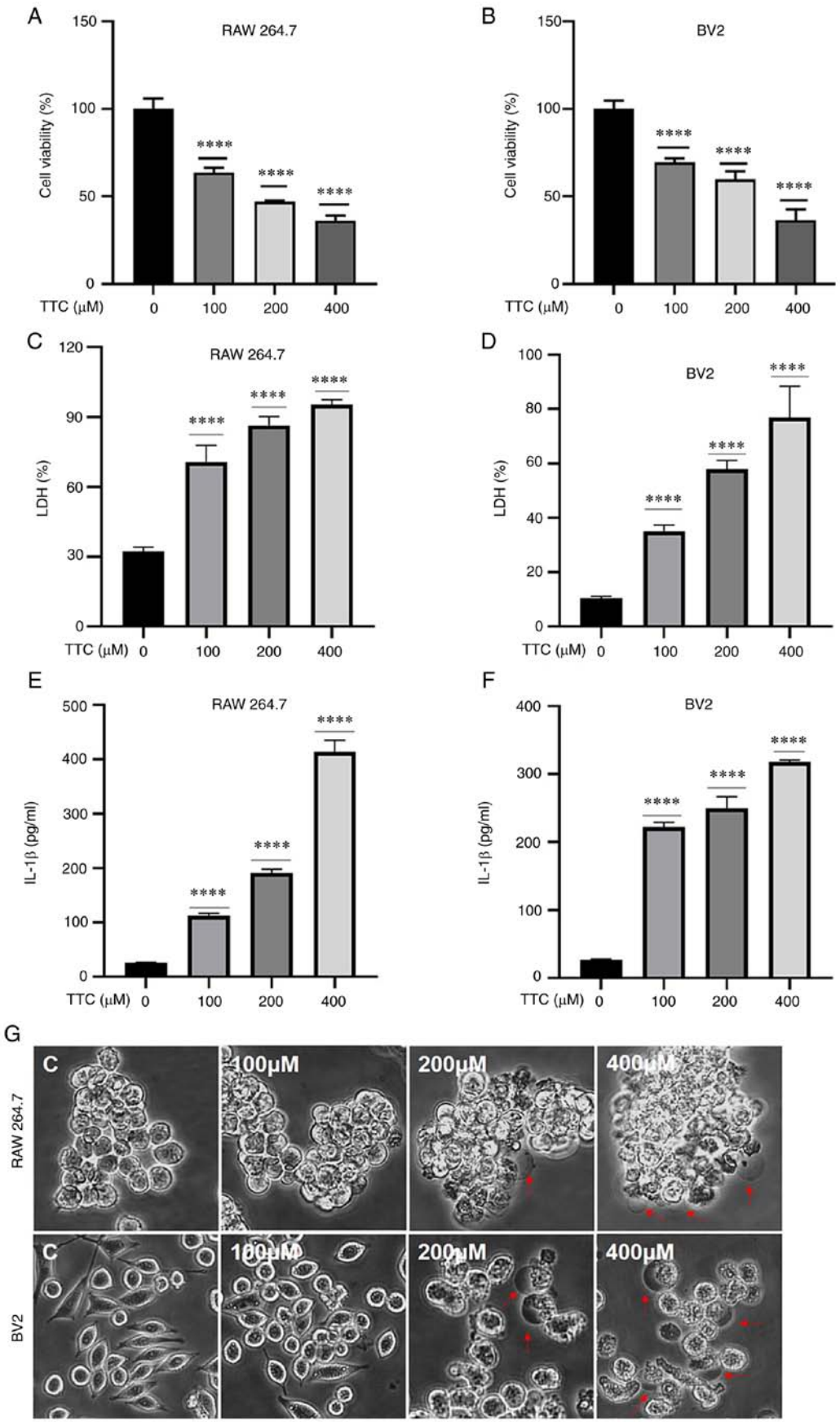

Figure 1. Effects of TTC on macrophages. RAW 264.7 and BV2 cells were treated with TTC at a range of concentrations for 24 h. The viability of TTC-treated (A) RAW 264.7 and (B) BV2 cells was determined using the Cell Counting Kit-8 assay. Release of LDH from TTC-treated (C) RAW 264.7 and (D) BV2 cells was measured using an LDH Cytotoxicity Assay Kit. Release of IL-1β from (E) RAW 264.7 and (F) BV2 cells was determined using a Mouse IL-1β ELISA Kit. (G) Morphology of RAW 264.7 and BV2 cells was monitored using light microcopy. The concentrations written on these images refer to the concentration of TTC used. The cells indicated by the red arrows are cells undergoing pyroptosis (magnification, x200). ****P<0.0001 vs. control. C, control; LDH, lactate dehydrogenase; TTC, tetracaine hydrochloride.

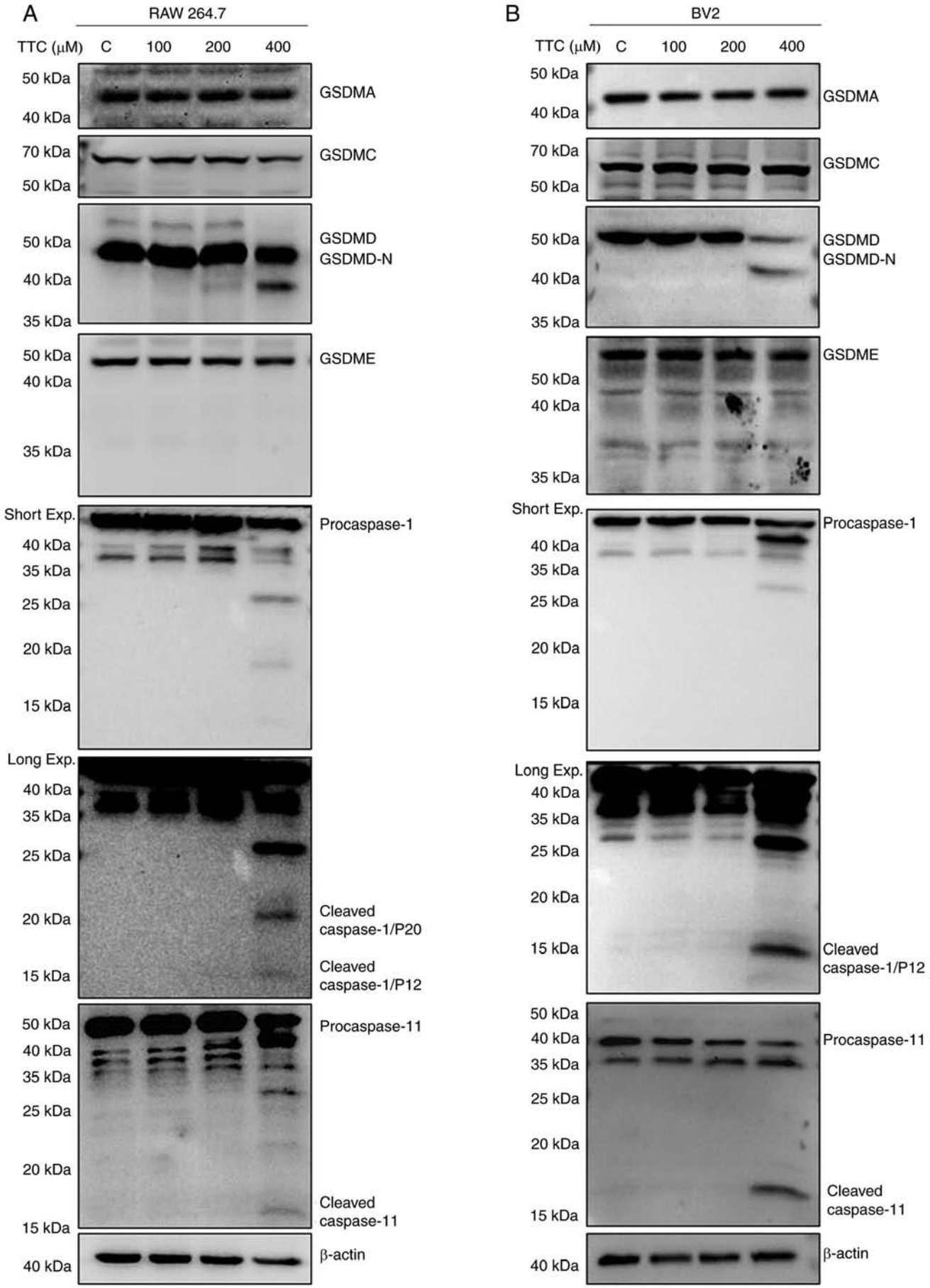

Figure 2. TTC induces pyroptosis through GSDMD via both canonical and non-canonical inflammatory pathways in macrophages. RAW 264.7 and BV2 cells were treated with TTC at a range of concentrations for 24 h. Protein expression levels of GSDMA, GSDMC, GSDMD, GSDME, caspase-1, caspase-11 and β-actin in (A) RAW 264.7 and (B) BV2 cells were determined by western blotting. TTC, tetracaine hydrochloride; GSDM, gasdermin; C, control.

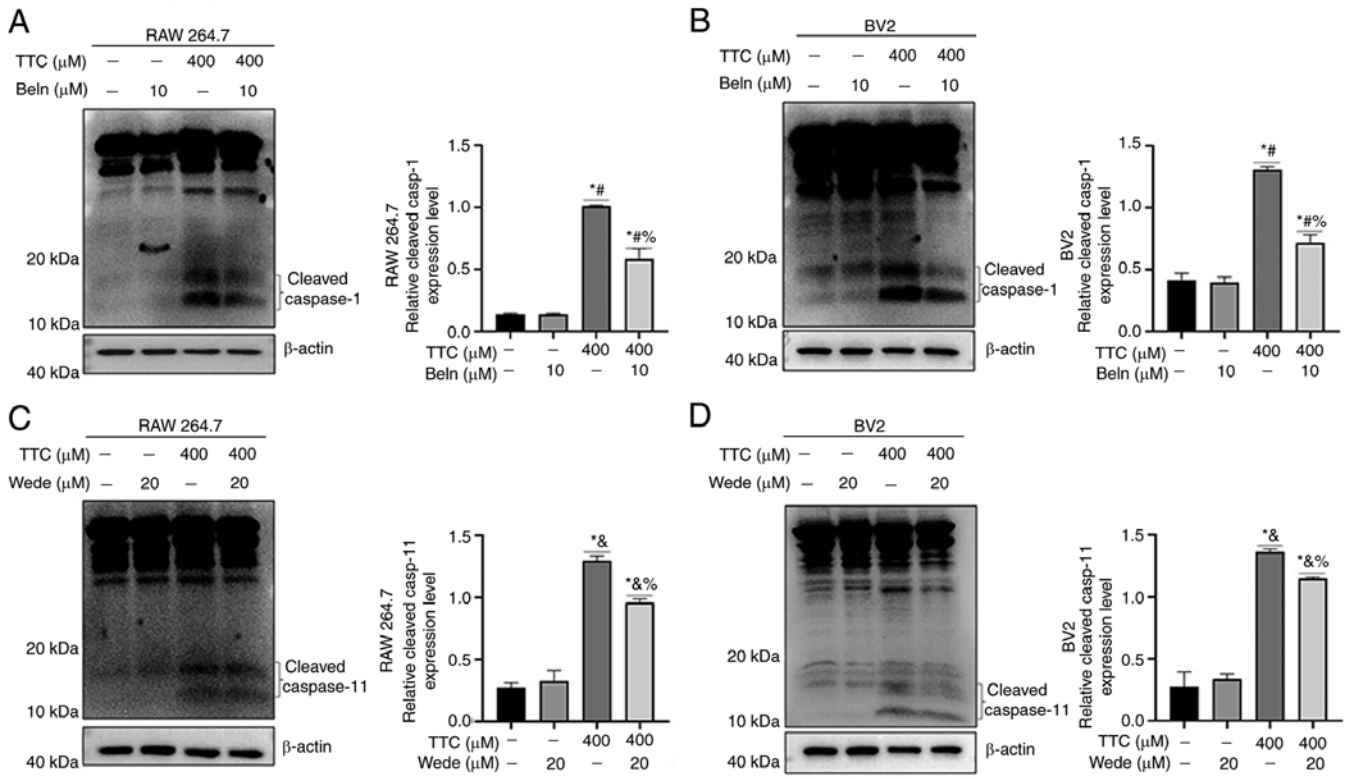

Figure 3. Effects of Beln and Wede on TTC-induced activation of caspase-1 and caspase-11 in macrophages. Caspase-1 protein expression levels were examined using western blotting in (A) RAW 264.7 and (B) BV2 cells pretreated with Beln for 30 min followed by 24 h treatment with TTC. Caspase-11 protein expression levels were examined using western blotting in (C) RAW 264.7 and (D) BV2 cells pretreated with Wede for 30 min followed by 24 h treatment with TTC. Protein expression levels were semi-quantified using ImageJ software. *P<0.05 vs. control; #P<0.05 vs. Beln group; &P<0.05 vs. Wede group; %P<0.05 vs. TTC group. TTC, tetracaine hydrochloride; Beln, Belnacasan; Wede, Wedelolaone.

were examined in the present study (Fig. 1C-F). These results demonstrated that the secretion of both LDH and IL-1β was significantly increased after TTC treatment and this effect was TTC-dose-dependent. As the release of LDH and IL-1β have been perceived as hallmarks of pyroptosis (15), combined with the morphological changes after TTC treatment, these results suggested that TTC could induce pyroptosis in RAW 264.7 and BV2 cells.

TTC induces macrophage pyroptosis mediated by GSDMD cleavage. The molecular mechanism by which TTC could induce macrophage pyroptosis was subsequently examined. It has previously been reported that the GSDM protein family is the dominant effector of pyroptosis (15). To determine which GSDM protein exerts TTC-induced pyroptosis, the protein expression levels and the cleavage status of the GSDM protein family (GSDMA, GSDMC, GSDMD and GSDME) in RAW 264.7 and BV2 cells were determined by western blotting (Fig. 2A and B). The full-length GSDMD protein expression levels were decreased, whereas GSDMD N-terminal fragment (GSDMD-N), the fragment that possesses the pore-forming activity, was increased in macrophages treated with 400 μM TTC. However, GSDMA, GSDMC and GSDME demonstrated no change in protein expression levels upon TTC treatment. These findings suggested that GSDMD, the most frequently reported effector of pyroptosis (18), could be involved in TTC-induced pyroptosis, and TTC may influence the cleavage of GSDMD, rather than its total expression. Therefore, TTC-induced macrophage pyroptosis may be mediated by GSDMD cleavage.

GSDMD cleavage is regulated by both caspase-1 and caspase-11 in TTC-induced macrophage pyroptosis. GSDMD-dependent pyroptosis is regulated through the canonical inflammasome pathway by caspase-1 activation, and the noncanonical inflammasome pathway by caspase-11 in mice and caspase-4/-5 in humans (18). In the present study, the involvement of GSDMD in TTC-induced pyroptosis was demonstrated; therefore, further examination of the expression of caspase-1 and caspase-11 by western blotting was performed (Fig. 2A and B). These results showed that the protein expression levels of both cleaved caspase-1 (P20 and P12) and caspase-11 were upregulated after TTC stimulation, suggesting the involvement of both canonical and non-canonical inflammatory pathways. Additionally, expression of cleaved caspase-3 was also upregulated by TTC (Fig. S1A and B), suggesting that TTC-induced cell death may be caused by apoptosis in addition to pyroptosis. This is consistent with a previous study that reported apoptosis as a major mechanism of cell death caused by TTC in HCEP cells (8).

To validate these results in the present study, cells were treated with the caspase-1 inhibitor Beln and the caspase-11 inhibitor Wede. The inhibitory activity of Beln and Wede on functional caspase-1 and caspase-11, respectively, was confirmed. The results demonstrated that Beln treatment alone had no significant effect on the protein expression

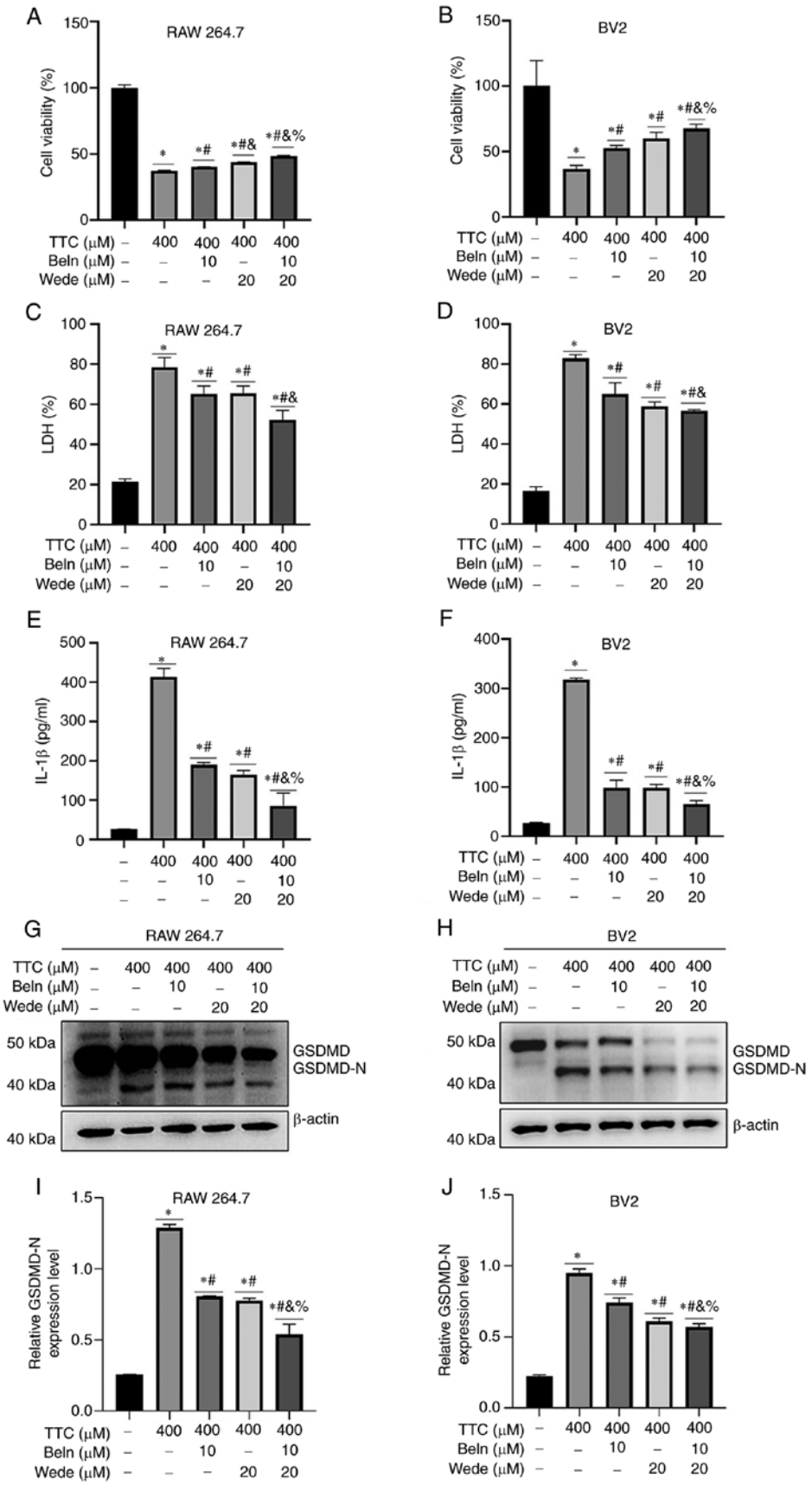

Figure 4. GSDMD-induced pyroptosis occurs via both canonical and non-canonical inflammatory pathways in TTC-treated macrophages. (A) RAW 264.7 and (B) BV2 cells were treated with 400 μM TTC for 24 h following pretreatment with or without Beln and/or Wede for 30 min. Cell viability was determined using the Cell Counting Kit-8 assay. Release of LDH from (C) RAW 264.7 and (D) BV2 cells was measured using an LDH Cytotoxicity Assay Kit. Release of IL-1β from (E) RAW 264.7 and (F) BV2 cells was determined using a Mouse IL-1β ELISA kit. Protein expression levels of GSDMD and β-actin in (G) RAW 264.7 and (H) BV2 cells was determined by western blotting. (I and J) Protein expression levels were semi-quantified using ImageJ software. *P<0.05 vs. control; $^{\#}$P<0.05 vs. TTC group; $^{\&}$P<0.05 vs. TTC + Beln group; $^{\%}$P<0.05 vs. TTC + Wede group. TTC, tetracaine hydrochloride; Beln, Belnacasan; Wede, Wedelolaone; GSDM, gasdermin.

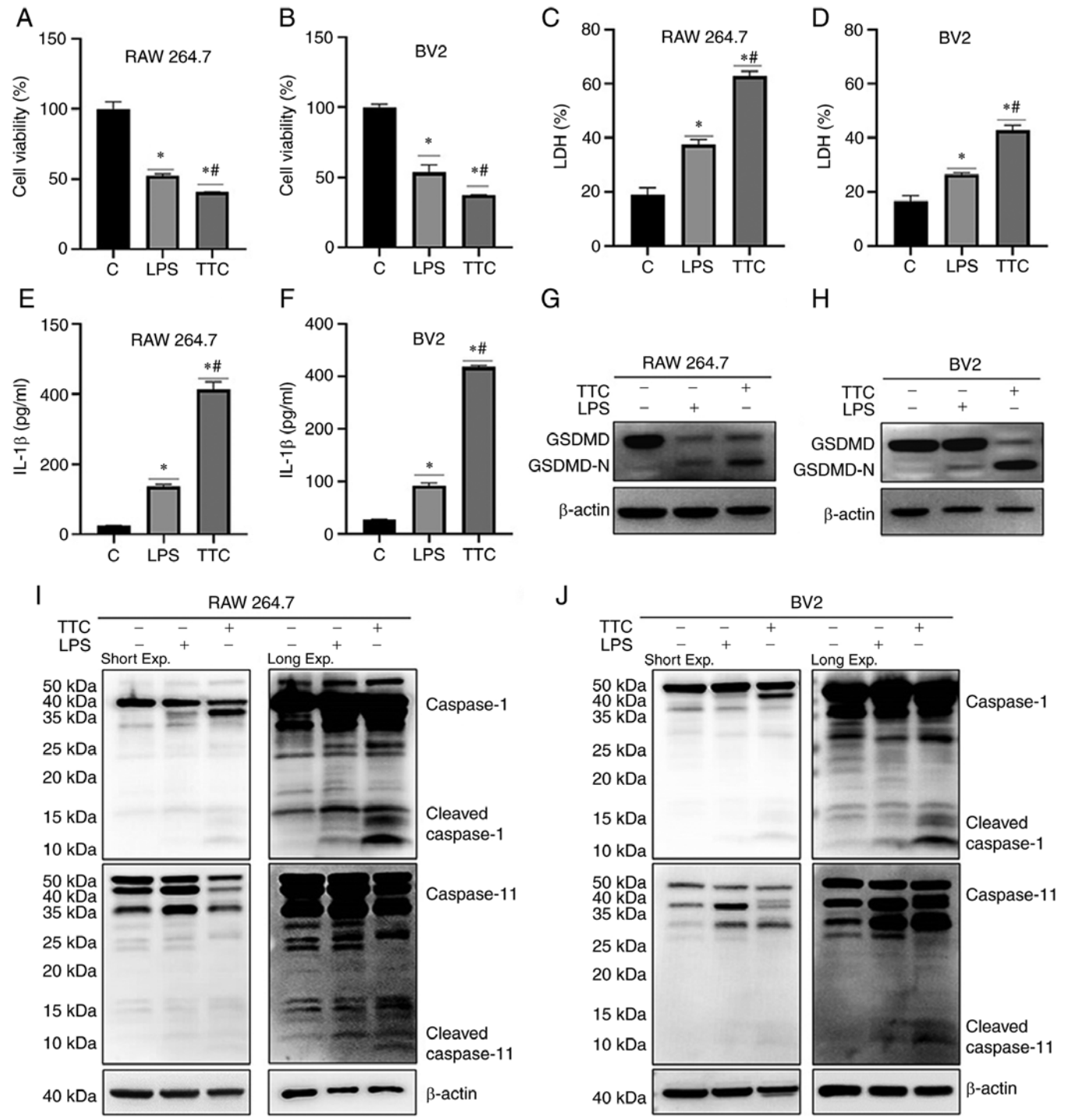

Figure 5. TTC-induced pyroptosis differed from LPS-induced pyroptosis in macrophages. RAW 264.7 and BV2 cells were treated with TTC and/or LPS for 24 h. Cell viability of (A) RAW 264.7 and (B) BV2 cells was determined using a Cell Counting Kit-8. Release of LDH from (C) RAW 264.7 and (D) BV2 cells was measured with LDH Cytotoxicity Assay Kit. Release of IL-1β from (E) RAW 264.7 and (F) BV2 cells was determined with a Mouse IL-1β ELISA Kit. Protein expression levels of GSDMD in (G) RAW 264.7 and (H) BV2 cells and, protein expression levels of caspase-1 and caspase-11 in (I) RAW 264.7 and (J) BV2 cells were determined using western blotting. *P<0.05 vs. control; #P<0.05 vs. LPS group. TTC, tetracaine hydrochloride; LPS, lipopolysaccharide; LDH, lactate dehydrogenase; exp, exposure; GSDM, gasdermin.

levels of caspase-1, but significantly decreased TTC-induced caspase-1 cleavage (Fig. 3A and B). Additionally, Wede caused a significant decrease in TTC-induced caspsase-11 cleavage (Fig. 3C and D). Inhibition of TTC-induced pyroptosis by Beln and Wede was examined by pretreating cells with the inhibitors for 30 min, followed by TTC exposure. These results demonstrated that both Beln and Wede significantly abrogated the decrease of cell viability (Fig. 4A and B), LDH release (Fig. 4C and D), IL-1β release (Fig. 4E and F) and the upregulation of GSDMD-N induced by TTC (Fig. 4G and H). Moreover, treatment of cells with both Beln and Wede significantly inhibited the vast majority of GSDMD expression, indicating a synergistic effect in reversing TTC-induced pyroptosis compared with treatment using a single inhibitor (Fig. 4G-J).

These results suggested that TTC-induced pyroptosis may be mediated by both canonical and non-canonical inflammatory pathways in macrophages.

Regulatory mechanisms underlying TTC-induced pyroptosis differ from LPS-induced pyroptosis in macrophages. LPS is known to induce pyroptosis in macrophages (27). In the present study, the mechanism of induction of macrophage pyroptosis by TTC and LPS were compared. The results showed that TTC or LPS treatment of both RAW 264.7 and BV2 cells demonstrated a significant decrease in cell viability (Fig. 5A and B), significant increases in the secretion of LDH (Fig. 5C and D) and IL-1β (Fig. 5E and F), and GSDMD cleavage (Fig. 5G and H). However, when caspase-1/11 was detected, both TTC and LPS could induce caspase-1/11 cleaveage, but the cleavage fragments were not the same (Fig. 5I and J). Compared with LPS, TTC treatment influenced caspase-1 and caspase-11 cleavage, rather than upregulating the whole protein. In addition, it was demonstrated that the cleaved fragments of caspase-1/-11 induced by TTC differed from those induced by LPS, as the cleavage fragments of caspase-1/-11 generated by TTC and LPS were located at different positions on the western blot membrane, suggesting the mechanism of TTC-induced pyroptosis might not be the same as that of LPS. Further investigation is required to identify the mechanism of action of the different cleavage pattern induced by TTC treatment demonstrated in the present study and how TTC interacts with these inflammatory caspases.

TTC induces pyroptosis in macrophages in vivo. Next, the potential for TTC to induce pyroptosis *in vivo* was investigated. TTC or an equal volume of physiological saline was intraperitoneally injected into mice and the PMs were extracted to analyze the protein expression levels of GSDMD. GSDMD-N was upregulated in PMs from the TTC group compared with control group, suggesting that TTC induced macrophage pyroptosis *in vivo* (Fig. 6).

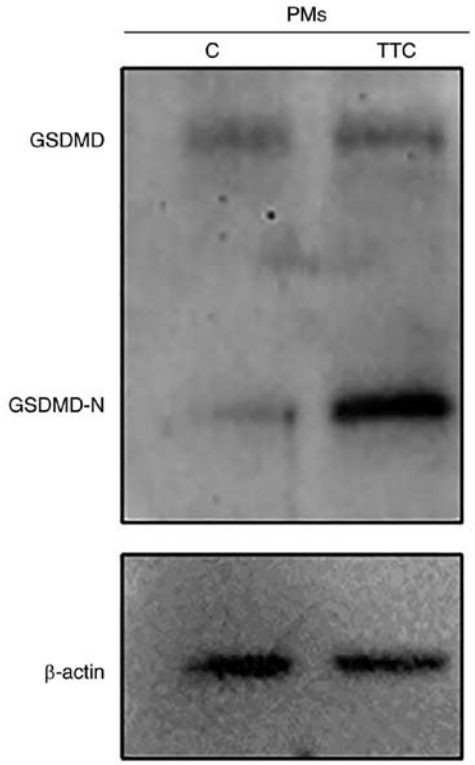

Figure 6. TTC induces pyroptosis in macrophages *in vivo*. Mice were intraperitoneally injected with TTC or PBS, then murine PMs were collected for western blotting. C, control, TTC, tetracaine hydrochloride; PM, peritoneal macrophage; GSDM, gasdermin.

Discussion

Previous studies have reported that TTC causes cytotoxicity in various cell types mainly through the induction of apoptosis, a type of PCD characterized by nuclear fragmentation, plasma membrane blebbing, cell shrinkage and formation of apoptotic bodies (7,8). The present study demonstrated that pyroptosis was the mechanism of cell death involved in TTC cytotoxicity (Fig. 7). Pyroptosis is a form of PCD characterized by the formation of a plasma membrane pore, swelling of the cell, swift plasma membrane disruption, and release of intracellular contents and pro-inflammatory cytokines. Although apoptosis and pyroptosis are different forms of PCD, certain pathological factors can induce both types of PCD as caspase-3 can cause a switch between apoptosis and pyroptosis (28).

In the present study, an increase in the release of IL-1β from macrophages treated with 100, 200 and 400 μM TTC was demonstrated, while the pyroptosis-related proteins GSDMD-N, caspase-1 and caspase-11 were only detected in macrophages treated with 400 μM TTC. However, caspase-1 and caspase-11 inhibitors, Wede and Beln, reduced IL-1β release, which suggests that the release of IL-1β is associated with caspase-1 and caspase-11 expression, but is not wholly dependent on these cytokines. A similar trend was demonstrated by LDH release from TTC-treated cells. These results suggested that TTC could induce multiple cell death patterns in macrophages. In addition, necroptosis, similar to pyroptosis, is a lytic, inflammatory type of PCD, which is mainly mediated by MLKL proteins, and is characterized by cellular swelling, membrane rupture and cytoplasmic and nuclear disintegration (29). Furthermore, ferroptosis is an additional type of PCD that involves lipid peroxidation caused by iron accumulation and is characterized by mitochondrial condensation, reduced mitochondrial cristae and increased membrane density (30). NETosis is a unique form of PCD that occurs in response to various pathogens, cytokines and other physiological stimuli, and is characterized by the release of decondensed chromatin and granular contents into the extracellular space, which can form web-like structures known as neutrophil extracellular traps (31). However, it is currently unknown whether these forms of PCD, including necroptosis, ferroptosis and NETosis, are involved in TTC induced-cytotoxicity, and further in-depth studies are required to elucidate these underlying molecular mechanisms.

Local anesthetics, such as lidocaine, and general anesthetics, such as propofol and sevoflurane, have previously been reported to affect cell viability (32). Certain anesthetics can affect cell pyroptosis and related molecular mechanisms (Table I) (32-41). Combined anesthesia refers to the simultaneous or sequential use of multiple anesthetic drugs or techniques during surgical procedures to achieve the desired anesthetic state; it involves the synergistic effects of different

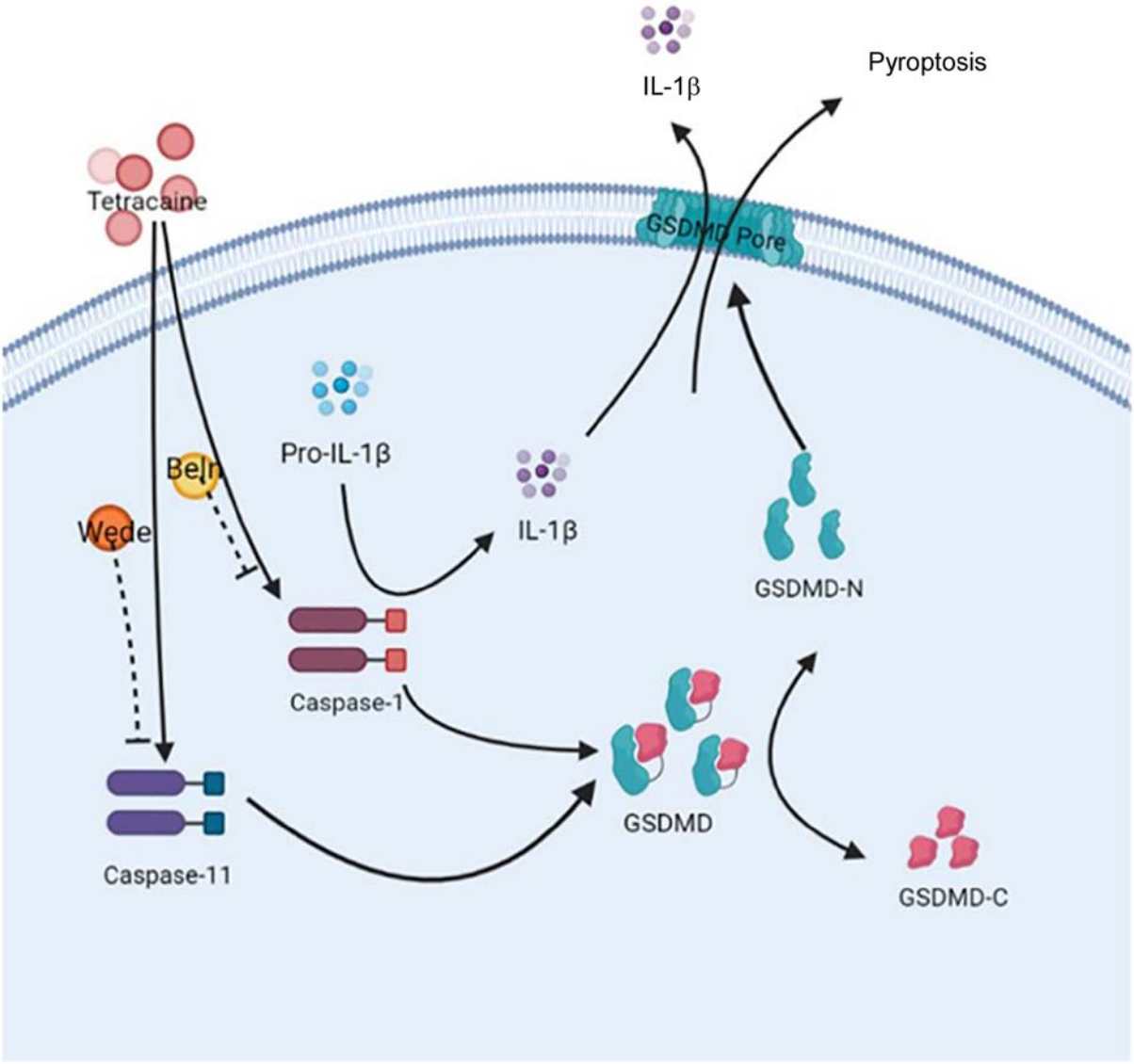

Figure 7. Schematic diagram of the mechanism of TTC-induced macrophage pyroptosis. TTC initiates the canonical and non-canonical inflammatory pathways by activating caspase-1 and caspase-11. Activated caspase-1 and caspase-11 cleave GSDMD into GSDMD-C and GSDMD-N. Then, GSDMD-N oligomerizes to form GSDMD pores on the cell membrane to induce pyropotosis in macrophages. IL-1β is activated by caspase-1 and released through the GSDMD pores (solid lines with arrows). The treatment of caspase-1 and caspase-11 inhibtors Beln and Wede could significantly decrease TTC-induced caspase-1 and caspase-11 cleavage, respectively, subsequently abrogating the upregulation of GSDMD-N and macrophagic pyrotosis induced by TTC (dashed line). TTC, tetracaine hydrochloride; GSDM, gasdermin; GSDMD-C, GSDMD C-terminal fragment; GSDMD-N, GSDMD N-terminal fragment.

drugs to enhance the effectiveness of anesthesia while minimizing side effects (42). Therefore, the different effects of certain anesthetics on the process of pyroptosis may provide some theoretical support for their use in combined anesthesia.

Activation of inflammatory caspases, such as murine or human caspase-1, or murine caspase-11 and its human homologs caspase-4/-5, preceding the induction of pyroptosis is a tightly regulated process (43,44). A previous study reported that caspase-1 is activated when the central scaffold of canonical inflammasomes, made of NLRP3, NLRP1, AIM2, NAIP-NLR4 and pyrin, detects its cognate ligands (45). Aberrant or excessive activation of caspase-1 can cause, or be associated with, certain autoinflammatory, autoimmune or metabolic diseases (44). In mice, the caspase-11 non-canonical inflammasome has been reported to sense infections caused by certain bacteria, such as *Escherichia coli*, *Salmonella* Typhimurium, *Legionella pneumophila* and *Burkholderia thailandensis*, by responding to the presence of cytoplasmic LPS (46). Additionally, caspase-11 activation serves an important role in the mediation of endotoxic shock and sepsis (47). In the present study, TTC-induced macrophage pyroptosis was demonstrated to be mediated through GSDMD cleavage by both caspase-1 and caspase-11. Furthermore, as the cleavage fragments of caspase-1/-11 generated after TTC and LPS treatment showed different patterns, the cleaved caspase-1 and caspase-11 caused by TTC and LPS may be different The mechanism of action of how TTC interacts with inflammatory caspases and whether it participates in other cellular pathways has yet to be explored. In addition, the alternative mechanism of TTC-induced macrophage pyroptosis demonstrated in the present study may influence the future development of therapeutics that

Table I. Effects of different anesthetics on the process of pyroptosis.

First author, year	Anesthetic	Tissue/cell type	Disease	Effect	Mechanism of action	(Refs.)
Ding *et al*, 2021	Lidocaine	Spinal cord	Spinal cord injury	Promotion	Upregulates NLRP3/ASC/caspase-1	(32)
Ding *et al*, 2021	Dexmedetomidine	Spinal cord	Spinal cord injury	Suppression	Inhibits priming and inflammasome activation, and reduces pyroptosis via protein kinase C-δ phosphorylation	(32)
Shi *et al*, 2022	Remimazolam	Brain	Cerebral I/R injury	Suppression	Inhibits NLRP3 inflammasome-dependent pyroptosis	(33)
Ye *et al*, 2018	Ketamine	Primary mouse hippocampal neuron	Hippocampal neurotoxicity	Promotion	Promotes NLRP3/caspase-1 complex recruitment to mitochondria	(34)
Li *et al*, 2022	Esketamine	Primary mouse astrocyte	POCD	Suppression	Inhibits pyroptosis-associated proteins via inhibition of the STING/TBK1 signaling pathway	(35)
Sun *et al*, 2019	Propofol	Bone marrow-derived macrophages, J774	Propofol infusion syndrome	Promotion	Activates NLRP3/ASC/caspase-1 pathway via mitochondrial reactive oxygen species	(36)
Liu *et al*, 2020		NR8383	Acute lung injury	Suppression	Inhibits the expression of pyroptotic proteins and enhances the expression of sirtuin 1	(37)
Dai *et al*, 2021	Sevoflurane	Primary rat hippocampal neuron	Neuroinflammation, neurocognitive impairment	Promotion	Activates NF-κB-mediated pyroptosis	(38)
Deng *et al*, 2022		AC16	I/R injury	Suppression	Activates the AMPK/ULK1 pathway to trigger autophagic flux and suppress NLRP3-mediated pyroptotic cell death	(39)
Chen *et al*, 2022		H19-7	Ischemic brain injury	Suppression	Regulates the Mafb/DUSP14 axis to mitigate oxygen-glucose deprivation-induced pyroptosis	(40)
Zheng *et al*, 2022		RAW 264.7	Acute lung injury	Suppression	Phosphorylates and activates the GSK-3β to suppress pyroptotic cell death	(41)

I/R, ischemia/reperfusion; POCD, postoperative cognitive dysfunction.

target pyroptosis. As GSDMD cleavage is definitive, the development of therapies targeting GSDMD may a better alternative than targeting inflammatory caspases.

Previous studies on the central nervous system toxicity of local anesthetics have focused on the effects of anesthetics on neurons as opposed to the immune system (11,12). The present study used the BV2 central nervous system immune cell line, which exerts a dual effect on neurons. As the present study demonstrated that TTC could cause BV2 pyroptosis, it could be suggested that TTC can indirectly exert toxic effects on neurons by inducing BV2 pyroptosis to release inflammatory factors, which can further trigger central nervous system toxicity Traditionally, benzodiazepines are used to antagonize the symptoms of local anesthetic poisoning by enhancing the inhibitory effects of γ-aminobutyric acid-ergic neurons in the limbic system (48). However, these drugs cause certain side effects, which in severe cases can affect the cognitive function of the patients (48). Presently used drugs such as disulfiram (49), dimethyl fumarate (50) and Prussian blue nanozyme (51) inhibit the pyroptotic pathway to alleviate diseases, such as familial Mediterranean fever, experimental autoimmune encephalitis and neurodegeneration. Hence, novel drugs that target the pyroptosis pathway could potentially provide a new future direction for the prevention and treatment of local anesthetic toxicity.

In conclusion, the present study demonstrated that the local anesthetic TTC induced macrophage pyroptosis through GSDMD cleavage and was mediated by both canonical and non-canonical inflammatory caspases. These results could potentially provide a promising strategy for the future prevention and treatment of local anesthetic toxicity.

Acknowledgements

Not applicable.

Funding

This study was supported by funding from the Sichuan Science and Technology Program (grant nos. 2022NSFSC1594 and 2022YFS0632), the Joint Foundation of Luzhou Government and Southwest Medical University (grant no. 2021LZXNYD-D08) and the Scientific Research Foundation of Southwest Medical University (grant no. 2021ZKZD011).

Availability of data and materials

The datasets used and/or analyzed during the current study are available from the corresponding author on reasonable request.

Authors' contributions

RZ and WG performed the experiments and drafted the manuscript. PY, ZQ, DZ, JJ and LL prepared materials, and collected and analyzed data. XJ and JF contributed to the design of the work, revised the manuscript and approved the final version of the manuscript to be published. All authors read and approved the final manuscript. RZ and JF confirm the authenticity of all the raw data.

Ethics approval and consent to participate

The study was approved by the Ethical Approval for Research Involving Animals in Southwest Medical University (Luzhou, China; approval no. SWMU20220028) and all animal experiments were performed according to the Guide for the Care and Use of Laboratory Animals of the National Institutes of Health.

Patient consent for publication

Not applicable.

Competing interests

The authors declare that they have no competing interests.

References

1. Wadlund DL: Local anesthetic systemic toxicity. AORN J 106: 367-377, 2017.
2. Macfarlane AJR, Gitman M, Bornstein KJ, El-Boghdadly K and Weinberg G: Updates in our understanding of local anaesthetic systemic toxicity: A narrative review. Anaesthesia 76 (Suppl 1): S27-S39, 2021.
3. Zhao W, Liu Z, Yu X, Lai L, Li H, Liu Z, Li L, Jiang S, Xia Z and Xu SY: iTRAQ proteomics analysis reveals that PI3K is highly associated with bupivacaine-induced neurotoxicity pathways. Proteomics 16: 564-575, 2016.
4. Yu XJ, Zhao W, Li YJ, Li FX, Liu ZJ, Xu HL, Lai LY, Xu R and Xu SY: Neurotoxicity comparison of two types of local anaesthetics: Amide-bupivacaine versus ester-procaine. Sci Rep 7: 45316, 2017.
5. Grant SA and Hoffman RS: Use of tetracaine, epinephrine, and cocaine as a topical anesthetic in the emergency department. Ann Emerg Med 21: 987-997, 1992.
6. Werdehausen R, Braun S, Fazeli S, Hermanns H, Hollmann MW, Bauer I and Stevens MF: Lipophilicity but not stereospecificity is a major determinant of local anaesthetic-induced cytotoxicity in human T-lymphoma cells. Eur J Anaesthesiol 29: 35-41, 2012.
7. Song Z and Fan TJ: Tetracaine induces apoptosis through a mitochondrion-dependent pathway in human corneal stromal cells in vitro. Cutan Ocul Toxicol 37: 350-358, 2018.
8. Pang X and Fan TJ: Cytotoxic effect and possible mechanisms of Tetracaine on human corneal epithelial cells in vitro. Int J Ophthalmol 9: 497-504, 2016.
9. Koizumi Y, Matsumoto M, Yamashita A, Tsuruta S, Ohtake T and Sakabe T: The effects of an AMPA receptor antagonist on the neurotoxicity of tetracaine intrathecally administered in rabbits. Anesth Analg 102: 930-936, 2006.
10. Barreda DR, Neely HR and Flajnik MF: Evolution of myeloid cells. Microbiol Spectr 4, 2016.
11. Mahajan A and Derian A: Local anesthetic toxicity. In: StatPearls StatPearls Publishing Copyright © 2023, StatPearls Publishing LLC., Treasure Island (FL) ineligible companies. Disclosure: Armen Derian declares no relevant financial relationships with ineligible companies, 2023.
12. Groban L: Central nervous system and cardiac effects from long-acting amide local anesthetic toxicity in the intact animal model. Reg Anesth Pain Med 28: 3-11, 2003.
13. Henn A, Lund S, Hedtjärn M, Schrattenholz A, Pörzgen P and Leist M: The suitability of BV2 cells as alternative model system for primary microglia cultures or for animal experiments examining brain inflammation. ALTEX 26: 83-94, 2009.
14. Gao W, Li Y, Liu X, Wang S, Mei P, Chen Z, Liu K, Li S, Xu XW, Gan J, *et al*: TRIM21 regulates pyroptotic cell death by promoting Gasdermin D oligomerization. Cell Death Differ 29: 439-450, 2022.
15. Orning P, Lien E and Fitzgerald KA: Gasdermins and their role in immunity and inflammation. J Exp Med 216: 2453-2465, 2019.
16. Broz P, Pelegrín P and Shao F: The gasdermins, a protein family executing cell death and inflammation. Nat Rev Immunol 20: 143-157, 2020.

17. Ding J, Wang K, Liu W, She Y, Sun Q, Shi J, Sun H, Wang DC and Shao F: Pore-forming activity and structural autoinhibition of the gasdermin family. Nature 535: 111-116, 2016.
18. Fang Y, Tian S, Pan Y, Li W, Wang Q, Tang Y, Yu T, Wu X, Shi Y, Ma P and Shu Y: Pyroptosis: A new frontier in cancer. Biomed Pharmacother 121: 109595, 2020.
19. Evavold CL, Ruan J, Tan Y, Xia S, Wu H and Kagan JC: The pore-forming protein gasdermin D regulates interleukin-1 secretion from living macrophages. Immunity 48: 35-44.e6, 2018.
20. Jorgensen I, Rayamajhi M and Miao EA: Programmed cell death as a defence against infection. Nat Rev Immunol 17: 151-164, 2017.
21. Zhang L, Xing R, Huang Z, Zhang N, Zhang L, Li X and Wang P: Inhibition of synovial macrophage pyroptosis alleviates synovitis and fibrosis in knee osteoarthritis. Mediators Inflamm 2019: 2165918, 2019.
22. Fisch D, Bando H, Clough B, Hornung V, Yamamoto M, Shenoy AR and Frickel EM: Human GBP1 is a microbe-specific gatekeeper of macrophage apoptosis and pyroptosis. EMBO J 38: e100926, 2019.
23. Frangogiannis NG: Regulation of the inflammatory response in cardiac repair. Circ Res 110: 159-173, 2012.
24. Zhang Y, Chen X, Gueydan C and Han J: Plasma membrane changes during programmed cell deaths. Cell Res 28: 9-21, 2018.
25. Scully AC and Boynton JR: Antibiotics and local anesthetics: Drug considerations for the child patient. J Mich Dent Assoc 99: 36-41, 71, 2017.
26. Kose AA, Karabaggli Y, Kiremitci A, Kocman E and Cetin C: Do local anesthetics have antibacterial effect on Staphylococcus aureus under in vivo conditions? An experimental study. Dermatol Surg 36: 848-852, 2010.
27. Liu Z, Wang M, Wang X, Bu Q, Wang Q, Su W, Li L, Zhou H and Lu L: XBP1 deficiency promotes hepatocyte pyroptosis by impairing mitophagy to activate mtDNA-cGAS-STING signaling in macrophages during acute liver injury. Redox Biol 52: 102305, 2022.
28. Wang Y, Gao W, Shi X, Ding J, Liu W, He H, Wang K and Shao F: Chemotherapy drugs induce pyroptosis through caspase-3 cleavage of a gasdermin. Nature 547: 99-103, 2017.
29. Bertheloot D, Latz E and Franklin BS: Necroptosis, pyroptosis and apoptosis: An intricate game of cell death. Cell Mol Immunol 18: 1106-1121, 2021.
30. Jiang X, Stockwell BR and Conrad M: Ferroptosis: Mechanisms, biology and role in disease. Nat Rev Mol Cell Biol 22: 266-282, 2021.
31. Moujalled D, Strasser A and Liddell JR: Molecular mechanisms of cell death in neurological diseases. Cell Death Differ 28: 2029-2044, 2021.
32. Ding XD, Cao YY, Li L and Zhao GY: Dexmedetomidine reduces the lidocaine-induced neurotoxicity by inhibiting inflammasome activation and reducing pyroptosis in rats. Biol Pharm Bull 44: 902-909, 2021.
33. Shi M, Chen J, Liu T, Dai W, Zhou Z, Chen L and Xie Y: Protective effects of remimazolam on cerebral ischemia/reperfusion injury in rats by inhibiting of NLRP3 inflammasome-dependent pyroptosis. Drug Des Devel Ther 16: 413-423, 2022.
34. Ye Z, Li Q, Guo Q, Xiong Y, Guo D, Yang H and Shu Y: Ketamine induces hippocampal apoptosis through a mechanism associated with the caspase-1 dependent pyroptosis. Neuropharmacology 128: 63-75, 2018.
35. Li Y, Wu ZY, Zheng WC, Wang JX, Yue-Xin, Song RX and Gao JG: Esketamine alleviates postoperative cognitive decline via stimulator of interferon genes/TANK-binding kinase 1 signaling pathway in aged rats. Brain Res Bull 187: 169-180, 2022.
36. Sun L, Ma W, Gao W, Xing Y, Chen L, Xia Z, Zhang Z and Dai Z: Propofol directly induces caspase-1-dependent macrophage pyroptosis through the NLRP3-ASC inflammasome. Cell Death Dis 10: 542, 2019.
37. Liu Z, Meng Y, Miao Y, Yu L and Yu Q: Propofol reduces renal ischemia/reperfusion-induced acute lung injury by stimulating sirtuin 1 and inhibiting pyroptosis. Aging (Albany NY) 13: 865-876, 2020.
38. Dai J, Li X, Wang C, Gu S, Dai L, Zhang J, Fan Y and Wu J: Repeated neonatal sevoflurane induced neurocognitive impairment through NF-κB-mediated pyroptosis. J Neuroinflammation 18: 180, 2021.
39. Deng L, Jiang L, Wei N, Zhang J and Wu X: Anesthetic sevoflurane simultaneously regulates autophagic flux and pyroptotic cell death-associated cellular inflammation in the hypoxic/re-oxygenated cardiomyocytes: Identification of sevoflurane as putative drug for the treatment of myocardial ischemia-reperfusion injury. Eur J Pharmacol 936: 175363, 2022.
40. Chen C, Zuo J and Zhang H: Sevoflurane post-treatment mitigates oxygen-glucose deprivationinduced pyroptosis of hippocampal neurons by regulating the Mafb/DUSP14 axis. Curr Neurovasc Res 19: 245-254, 2022.
41. Zheng F, Wu X, Zhang J and Fu Z: Sevoflurane suppresses NLRP3 inflammasome-mediated pyroptotic cell death to attenuate lipopolysaccharide-induced acute lung injury through inducing GSK-3β phosphorylation and activation. Int Immunopharmacol 109: 108800, 2022.
42. Litz RJ, Bleyl JU, Frank M and Albrecht DM: Combined anesthesia procedures. Anaesthesist 48: 359-372, 1999 (In German).
43. Kayagaki N, Stowe IB, Lee BL, O'Rourke K, Anderson K, Warming S, Cuellar T, Haley B, Roose-Girma M, Phung QT, *et al*: Caspase-11 cleaves gasdermin D for non-canonical inflammasome signalling. Nature 526: 666-671, 2015.
44. Shi J, Zhao Y, Wang K, Shi X, Wang Y, Huang H, Zhuang Y, Cai T, Wang F and Shao F: Cleavage of GSDMD by inflammatory caspases determines pyroptotic cell death. Nature 526: 660-665, 2015.
45. Lamkanfi M and Dixit VM: Mechanisms and functions of inflammasomes. Cell 157: 1013-1022, 2014.
46. Shi J, Zhao Y, Wang Y, Gao W, Ding J, Li P, Hu L and Shao F: Inflammatory caspases are innate immune receptors for intracellular LPS. Nature 514: 187-192, 2014.
47. Hagar JA, Powell DA, Aachoui Y, Ernst RK and Miao EA: Cytoplasmic LPS activates caspase-11: Implications in TLR4-independent endotoxic shock. Science 341: 1250-1253, 2013.
48. Dickerson DM and Apfelbaum JL: Local anesthetic systemic toxicity. Aesthet Surg J 34: 1111-1119, 2014.
49. Hu JJ, Liu X, Xia S, Zhang Z, Zhang Y, Zhao J, Ruan J, Luo X, Lou X, Bai Y, *et al*: FDA-approved disulfiram inhibits pyroptosis by blocking gasdermin D pore formation. Nat Immunol 21: 736-745, 2020.
50. Humphries F, Shmuel-Galia L, Ketelut-Carneiro N, Li S, Wang B, Nemmara VV, Wilson R, Jiang Z, Khalighinejad F, Muneeruddin K, *et al*: Succination inactivates gasdermin D and blocks pyroptosis. Science 369: 1633-1637, 2020.
51. Ma X, Hao J, Wu J, Li Y, Cai X and Zheng Y: Prussian blue nanozyme as a pyroptosis inhibitor alleviates neurodegeneration. Adv Mater 34: e2106723, 2022.